Design Oriented Stress-Strain Models for Engineered Cementitious Composites

Modelos de Diseño Orientado a Tensión-deformación para Hormigón Flexible

Madappa V.R. Sivasubramanian (Main author and Contact author)
National Institute of Technology Puducherry. Department of Civil Engineering, Puducherry, India.
Tiruvettakudi Village, Karaikal-609 609, Puducherry UT, India.
madappa@nitpy.ac.in

Shamsher Bahadur Singh
Birla Institute of Technology and Science Pilani. Department of Civil Engineering, Rajasthan, India
sbsingh@bits-pilani.ac.in

Narendran Rajagopalan
National Institute of Technology Puducherry. Department of Computer Science and Engineering, Puducherry, India.
narendran@nitpy.ac.in

Manuscript Code: 682
Date of Acceptance/Reception: 03.08.2016/07.09.2015

Abstract
Engineered Cementitious Composite (ECC) is known for multiple cracking and strain hardening property when loaded in tension. To incorporate this superior property in the design of structural elements, it is mandatory to develop design oriented stress-strain models considering the tensile strain hardening property. In the present study, stress-strain models are developed for both tension and compression using the empirical values available in literature. An analytical study has been conducted on the flexural response of Fiber Reinforced Polymer (FRP) reinforced ECC beams to understand the robustness of the developed stress-strain models. For this purpose, a special purpose non-linear computer program is developed based on force equilibrium and strain compatibility conditions to predict the ultimate load and deflection. The accuracy of the nonlinear computer program is validated by comparing the analytical results with experimental results available in literature which is found to be in close agreement. Hence, it is inferred that the developed stress-strain models can be used for various design purposes.

Keywords: Design, stress-strain, engineered cementitious composites, load, deflection

Resumen
El Hormigón Flexible (ECC) es conocido por múltiples grietas y propiedades de tensión de endurecimiento cuando está sometido a tensión. Para incorporar esta propiedad superior en el diseño de elementos estructurales, es obligatorio desarrollar modelos orientados al diseño de tensión-deformación teniendo en cuenta la propiedad de deformación de endurecimiento por tracción. En el presente estudio, los modelos de tensión-deformación se desarrollan tanto para tensión y compresión utilizando los valores empíricos disponibles en la literatura. Un estudio analítico se ha realizado acerca de la respuesta a la flexión de vigas de ECC de fibra de polímero reforzado (FRP), para entender la robustez del los modelos de tensión-deformación desarrollados. Para este propósito, un software no lineal de propósitos especiales se desarrolló sobre la base de las condiciones de equilibrio de fuerza y de compatibilidad de tensión para predecir la carga de rotura y deformación final. La precisión del programa de ordenador no lineal se validó mediante la comparación de los resultados analíticos con los resultados experimentales disponibles en la literatura encontrándose similitudes. Por lo tanto, se infiere que los desarrollos de modelos de tensión-deformación se pueden utilizar para diversos fines de diseño.

Palabras clave: Diseño, tensión-deformación, hormigón flexible, carga, deformación.

Introduction

Engineered Cementitious Composites (ECC) is a cement matrix based composite material which contains micro structurally tailored polymeric fibers such as polyethylene (PE) and polyvinyl alcohol (PVA) in stochastic orientation (Kanda & Li, 1999). The fiber volume fraction of ECC is typically 2% or less. It is a class of High Performance Fiber Reinforced Cementitious Composites (HPFRCC) which is based on micromechanics. In uni-axial loading, ECC shows ultra-high tensile strain capacity (2%-3%), with multiple microcracks during the inelastic deformation (Kanda & Li, 1999). ECC exhibits isotropic properties and can be prepared by normal mixing. The ultra-high ductility of ECC is exploited in earthquake resistant structures. Further, ECC can be applied to all kind of flexural and shear elements to carry higher tensile loads. ECC can be applied to all beam-column joints and plastic hinge zones to undergo inelastic deformation by absorbing more energy.

Rokugo, Kunieda, Kamada, Fujimoto & Furukawa (2002) investigated the flexural behavior of steel pipes surrounded by ECC and plates made of ECC. This experimental study also used plain mortar, steel fiber reinforced mortar for relative studies. The results of this study have shown that ECC specimens have shown greater ductile performance than other specimens which used plain mortar or steel fiber reinforced mortar.

Li & Wang (2002) conducted an experimental investigation on response of Glass Fiber-Reinforced Polymer (GFRP) reinforced ECC beam. This study demonstrated the higher load carrying capacity of ECC in flexure. GFRP reinforced ECC beam have shown better flexural response than GFRP reinforced concrete beam in terms of load carrying capacity and ductility. Moreover, it was also shown that ECC beams exhibit better shear performance than concrete beams with dense steel stirrups which suggests the elimination of the shear reinforcement is possible when concrete matrix is replaced by ECC.

Han, Feenstra & Billington (2003) developed a material constitutive model based on total strain method to analyse the structural elements made of ECC. The simulation results showed that implemented model was robust and reasonably accurate in simulating ECC structural components reinforced with steel and fiber-reinforced polymer bars. Li & Lepech (2006) suggested general design assumptions for reinforced ECC structures. They emphasised on the tensile load carrying capacity of ECC during inelastic strain hardening deformation. Assumptions regarding the shape of the tensile stress-strain relation, usable tensile and compressive strains are also addressed. Pan & Yuan (2013) conducted an experimental study on flexural response of FRP reinforced ECC beams and concluded that the FRP reinforced ECC beams show better flexural properties in terms of load carrying capacity, shear resistance, ductility, and damage tolerance compared with FRP reinforced concrete beams.

In the present study, design oriented stress-strain models are developed for ECC both in tension and compression. To understand the robustness of the developed models, an analytical study was carried out on flexural analysis of FRP reinforced ECC beams. To perform this study, associated stress block parameters for newly developed models are also derived and used in the analysis. The robustness of the developed stress-strain models is observed from the results of the present study which is verified against the experimental results available in Li &Wang (2002) and Pan & Yuan (2013) for three different beam specimens.

Research Scope

Ductility is the critical parameter in the design of concrete structures. It is anticipated that, the ECC will give promising properties such as high flexural strength, ultra-high ductility and enhanced durability to the structures. Development of stress-strain models for ECC by incorporating ultra-high ductility is a significant and appropriate step in the analysis and design of ECC structures.

Tensile Stress-Strain Model

Present study has proposed a tensile stress-strain model for ECC based on experimental data obtained from literature. For developing this model, the authors have selected six different experimental tensile stress-strains behaviours (Kanda & Li, 1999).The proposed tensile stress-strain model (Figure 1) is given by equations 1 & 2.

$$\left(\frac{f_t}{f_t^{'}}\right) = 134.75\left(\frac{\varepsilon_t}{\varepsilon_{tu}}\right) \quad \text{if} \quad \frac{\varepsilon_t}{\varepsilon_{tu}} < 0.00545 \qquad (1)$$

$$\left(\frac{f_t}{f_t^{'}}\right) = 0.2371\left(\frac{\varepsilon_t}{\varepsilon_{tu}}\right) + 0.7334 \text{ if } 0.00545 < \frac{\varepsilon_t}{\varepsilon_{tu}} < 1 \qquad (2)$$

where, $f_t =$ tensile stress at each loading stage; $f_t^{'} =$ peak tensile stress (ultimate tensile strength); $\varepsilon_t =$ tensile strain at each loading stage; $\varepsilon_{tu} =$ peak tensile strain (ultimate tensile strain capacity).

Figure 1. Tensile stress-strain model for PE-ECC. Source: Self-elaboration.

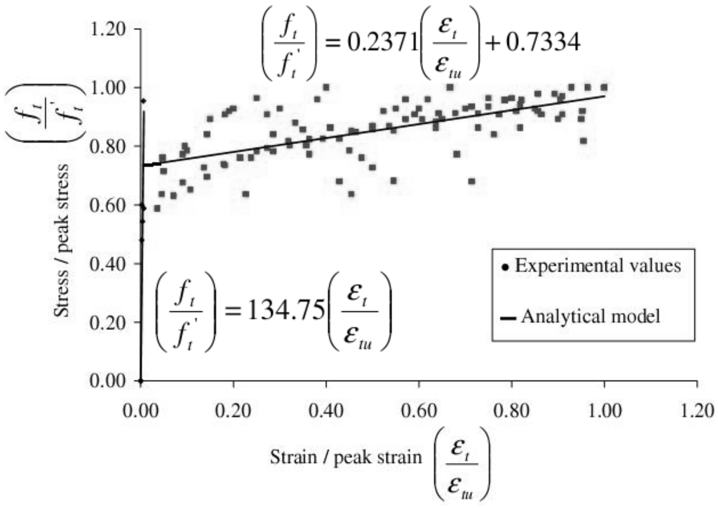

Compressive Stress-Strain Model

An experimental investigation (Li & Wang, 2002) shows that ECC has high ultimate compressive strain capacity than concrete. A bi-linear compression model proposed by Maalej & Li (1995) gives better understanding about compression behaviour of ECC. With these experimental investigations and existing behaviours, authors have made an attempt to develop an empirical stress-strain model of ECC in compression. The experimental values are taken from the literature (Li & Wang, 2002, Maalej & Li, 1995). Since the post-peak behaviour of ECC in uniaxial compression is a sudden drop (up to 40% of its peak strength), the present model is comprised the behaviour only up to peak point. The developed empirical model (Figure 2) is expressed by Equation 3.

$$\left(\frac{f_c}{f_c^{'}}\right) = 1.64\left(\frac{\varepsilon_c}{\varepsilon_{cu}}\right) - 0.65\left(\frac{\varepsilon_c}{\varepsilon_{cu}}\right)^2 \qquad (3)$$

where, $f_c =$ compressive stress at each loading stage; $f_c^{'} =$ peak compressive stress (ultimate compressive strength); $\varepsilon_c =$ compressive strain at each loading stage; $\varepsilon_{cu} =$ peak compressive strain (ultimate compressive strain).

Figure 2. Compressive stress-strain model for PE-ECC. Source: Self-elaboration.

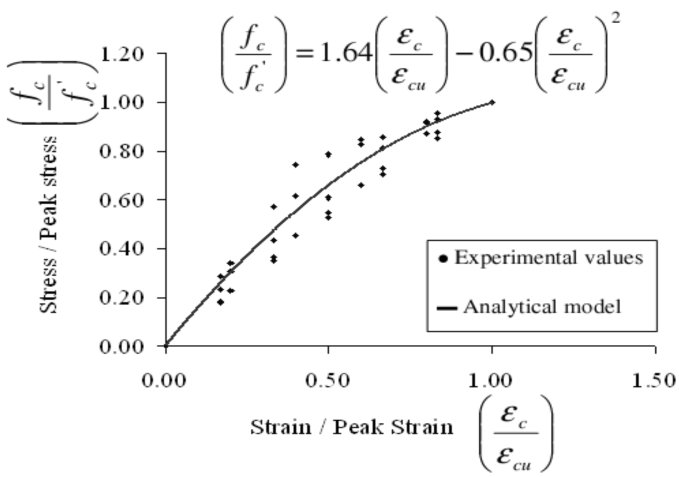

It was experimentally proved that the pseudo-tensile strain hardening property of ECC will increase the moment carrying capacity and ductility of the section reinforced with FRP bars (Li & Wang, 2002; Yuan & Pan, 2013). To incorporate the pseudo-tensile strain hardening, it is necessary that the actual stress-strain distribution should be modelled as simple rectangular block. The stress block parameters can be determined by equating the resultant tensile force and its location obtained from stress-strain relation to that obtained by equivalent stress block. Equation 4 expresses the resultant tensile force, while Equation 5 can be used to locate the centroid of resultant tensile force (Figure 3).

Figure 3. Stress-strain distribution across the section of the beam. Source: Self-elaboration.

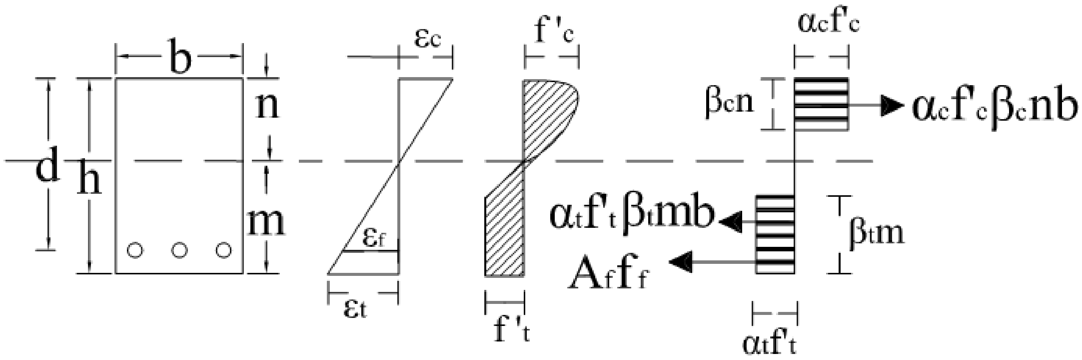

(A) Cross-section **(B)** Strain **(C)** Stress **(D)** Stress-block

$$\int_{o}^{m} f_t b dy = \alpha_t f_t^{'} \beta_t mb \text{ where } m = (h-n) \quad (4) \qquad y_t = \frac{\int_0^m f_t bydy}{\int_0^m f_t bdy} \quad (5)$$

where,

$h =$ overall depth of the beam section; $n =$ depth of neutral axis section; $b =$ width of the beam, $\alpha_t =$ ratio of average tensile stress to the peak tensile strength of ECC; $\beta_t =$ ratio of the depth of tensile stress block to the depth of the section below neutral axis. Equations 6 and 7 will give the stress block parameters

when, $0 < \dfrac{\varepsilon_t}{\varepsilon_{tu}} < 0.00545$

$$\alpha_t = 101.06\left(\frac{\varepsilon_t}{\varepsilon_{tu}}\right) \quad (6.a)$$

$$\beta_t = 0.6667 \quad (7.a)$$

where,

$$\alpha_t \beta_t = \left(\frac{c_1 + c_3}{f_t^{'} m}\right) \quad (6.b)$$

$$\beta_t = 2 - \left(\frac{2}{m}\right) \times \left(\frac{c_2 \times c_1 + c_6 \times c_3}{c_1 + c_3}\right) \quad (7.b)$$

$c_1 = 0.5 \times f_1 \times d_1$; $c_2 = 0.667 \times d_1$;

$c_3 = \left[f_1 \times d_2 + 0.5 \times d_2 \times (f_2 - f_1)\right]$;

$$c_4 = \frac{d_2}{3} \times \left[1 + \frac{f_1}{f_1 + f_2}\right]$$

$c_5 = d_4 - c_4$; $c_6 = c_5 + d_1$.

when, $0.00545 < \frac{\varepsilon_t}{\varepsilon_{tu}} < 1$

$$f_1 = 0.7343 f_t^{'} ; \quad f_2 = \left[0.2371 \left(\frac{\varepsilon_t}{\varepsilon_{tu}} \right) + 0.7334 \right] \times f_t^{i}$$

$$d_1 = 0.00545 \times \left(\frac{\varepsilon_t}{\varepsilon_{tu}} \right) \times m ; \quad d_2 = m - d_1$$

Further, it is also required to approximate the actual compression behavior of ECC as simple rectangular stress block. The stress block parameters can be calculated by equating the resultant compression force and its location obtained from nonlinear stress-strain relation to that obtained by equivalent stress block. Equation 8 expresses the resultant compressive force, while Equation 9 can be used to locate the centroid of resultant compressive force.

$$\int_o^n f_c b dy = \alpha_c f_c^{'} \beta_c n b \qquad (8)$$

$$y_c = \frac{\int_0^n f_c b y dy}{\int_0^n f_c b dy} \qquad (9)$$

where,

$\alpha_c =$ ratio of average compressive stress to the peak compressive strength of ECC; $\beta_c =$ ratio of the depth of compressive stress block to the depth of neutral axis. Using Equations 10 & 11 the stress block parameters can be evaluated.

$$\alpha_c \beta_c = 0.82 \left(\frac{\varepsilon_c}{\varepsilon_{cu}} \right) - 0.216 \left(\frac{\varepsilon_c}{\varepsilon_{cu}} \right)^2 \qquad (10)$$

$$\beta_c = \frac{0.5468 - 0.107 \left(\frac{\varepsilon_c}{\varepsilon_{cu}} \right)}{0.82 - 0.216 \left(\frac{\varepsilon_c}{\varepsilon_{cu}} \right)} \qquad (11)$$

Robustness of Developed Models

To understand the robustness of the developed stress-strain models and derived stress block parameters, an analytical study was carried out on flexural response of FRP reinforced ECC beams. The following assumptions are made while performing the flexural analysis; 1. behavior of ECC is nonlinear and bilinear in compression and tension, respectively, 2. behavior of FRP bar is linear elastic till rupture, 3. bond between the FRP rods and ECC material is perfect, 4. ECC fails when it reaches the ultimate strain value in compression, 5. FRP bar ruptures when it reaches the rupture strain value, 6. behavior of ECC is modeled as simple rectangular blocks both in compression and tension, respectively. A special purpose nonlinear computer program was developed to predict the analytical load vs. deflection response using MATLAB 7.0.1 (Figure 4). The load versus deflection response consists of two parts (a) linear response (b) nonlinear response. This computer program is using fundamental linear elastic theory to predict the linear response. The nonlinear response is predicted based on strain controlled approach using equilibrium of forces and compatibility of strain (Singh, 2015). This program considers tensile strain hardening behavior of ECC and incorporates the tensile load carrying capacity. For a trial strain levels in compression and tension, neutral axis depth and forces are evaluated. If tensile and compressive forces satisfy the force equilibrium equation, then the assumed strains and corresponding neutral axis depth are correct and used for curvature prediction. The midspan deflection of the beam is computed by numerical integration of the curvature of the beam along its length. Analytical flexural load vs. deflection response has been evaluated for three different beam specimens and compared with experimental results obtained from literature (Li & Wang, 2002; Pan & Yuan, 2013). Complete details about the material characteristics and test setup of the experimental program of Li & Wang (2002) and Pan & Yuan (2013) with which analytical results are compared are discussed below.

Figure 4. Logic flowchart of the special purpose non-linear computer program. Source: Self-elaboration.

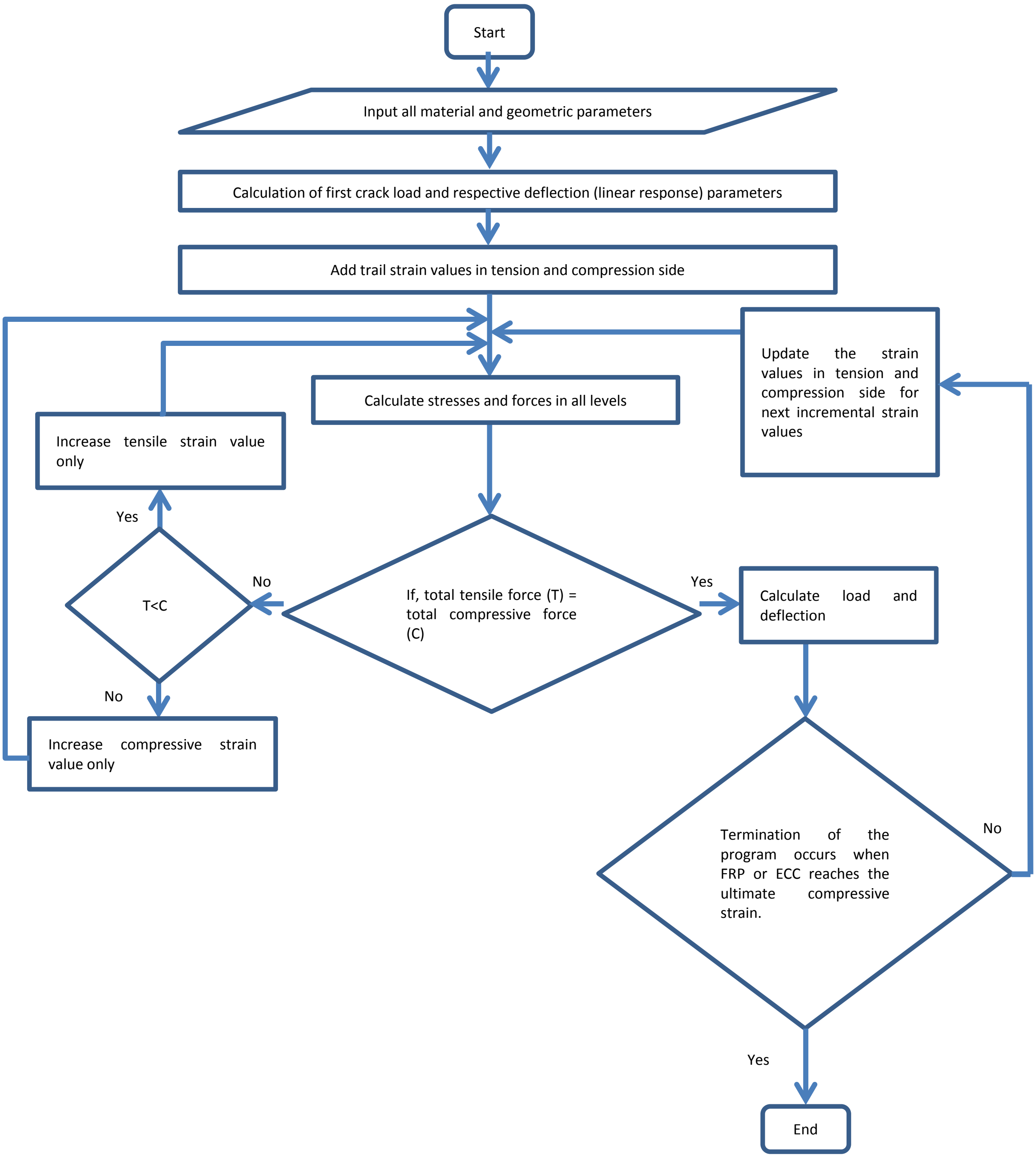

Material Properties

The FRP reinforcing bars used in literature are Glass FRP (GFRP) and Basalt FRP (BFRP) rods. The reinforcing bar has spiral-wrapped glass fiber braid to provide lateral confinement, and a coarse silica sand-coated surface to enhance bonding with the ECC mix. The mechanical and design properties of the GFRP and BFRP rods are given in Table 1. The mechanical and design properties of ECC matrix in uniaxial tension and in uniaxial compression are given in Table 2 and Table 3, respectively.

Table 1. FRP reinforcing bar properties. Source: Self-elaboration.

Literature	Type of FRP bar used	Bar diameter, mm	Tensile elasticity modulus, GPa	Ultimate tensile strength, MPa	Ultimate rupture strain, %
Li and Wang (2002)	GFRP	12.9	40	740	1.9
Yun and Pan (2012)	BFRP	20	46.2	907	1.96

Table 2. ECC matrix properties in uni-axial tension. Source: Self-elaboration.

Literature	First crack strength, MPa	Ultimate tensile strength, MPa	Ultimate strain capacity, %
Li and Wang (2002)	3	8	3.5
Yun and Pan (2012)	3.5	5	4

Table 3. ECC matrix properties in uni-axial compression. Source: Self-elaboration.

Literature	Beam designation	Ultimate compressive strength, MPa	Ultimate compressive strain, %
Li and Wang (2002)	GRE16-3R	76.2	0.53
	GRE16	71.2	0.53
Yun and Pan (2012)	BRE 20	38.3	0.25

Test Specimens

The experimental study conducted by Li & Wang (2002) and Pan & Yuan (2013) tested many RC beams with various combinations. Since the present study deals with flexural behavior of FRP reinforced ECC beams, details are given for three beam specimens. Beam specimens are chosen with actual reinforcement ratio 1.05 % to 2.73 % covering all failure modes such as tension and compression failure. GRE16-3R and GRE16 are beam specimens chosen from Li & Wang (2002). Beam specimen BRE 20 is chosen from Pan & Yuan (2013). Summary of the beam specimens are shown Table 4.

Table 4. Summary of beams specimens. Source: Self-Elaboration.

Literature	Beam designation	Effective length, mm	Reinforcement ratio, %	Cross sectional details (mm x mm)	Effective depth (mm)
Li and Wang (2002)	GRE16	1500	1.82	114 x 153	25
	GRE16-3R	1500	2.73	114 x 153	25
Yun and Pan (2012)	BRE 20	2050	1.05	180 x 300	45

Test Procedure

All the three beams were tested for zero to ultimate load and were subjected to one cycle of the loading process. The loading pattern is two point loading. The distance between the two loading points is 242 and 350 mm in the study of Li & Wang (2002) and Pan & Yuan (2012), respectively.

Load vs. Deflection Curves

Further, using developed computer program, load vs. midspan deflection behavior is plotted for all the three beam specimens. Since GRE 16 failed in flexural tension (during the experiment), the curtailment of the simulation is governed by rupture strain of GFRP bars. In the case of GRE 16-3R and BRE 20 beams failed in flexural compression, the curtailment of simulation is governed by the ultimate flexural compressive strain. In general, for all the three beams, the analytical load vs. deflection response is in close agreement with the experimental response as shown in Figures 5, 6 & 7. The results of the comparative study are given in Table 5. For the beam GRE 16, the difference is 11.6% and 1.6% in the case of load capacity and deflection, respectively. For the beam GRE 16-3R, the difference is 2.5% and 11% in the case of load capacity and deflection, respectively. For the beam BRE 20, the difference is 2.34 % and 2.56%, in the case of load capacity and deflection, respectively.

Table 5. Summary of comparative study details. Source: Self-elaboration.

Literature	Beam designation	Analytical		Experimental	
		Peak load, kN	Midspan deflection, mm	Peak load, kN	Midspan deflection, mm
Li and Wang (2002)	GRE16	87	44	76.9	43.3
	GRE16-3R	102	37.1	104.6	42
Yun and Pan (2012)	BRE 20	243.2	35.1	237.5	37

Figure 5. Comparison of Load-Deflection of beam specimen GRE 16. Source: Self-elaboration.

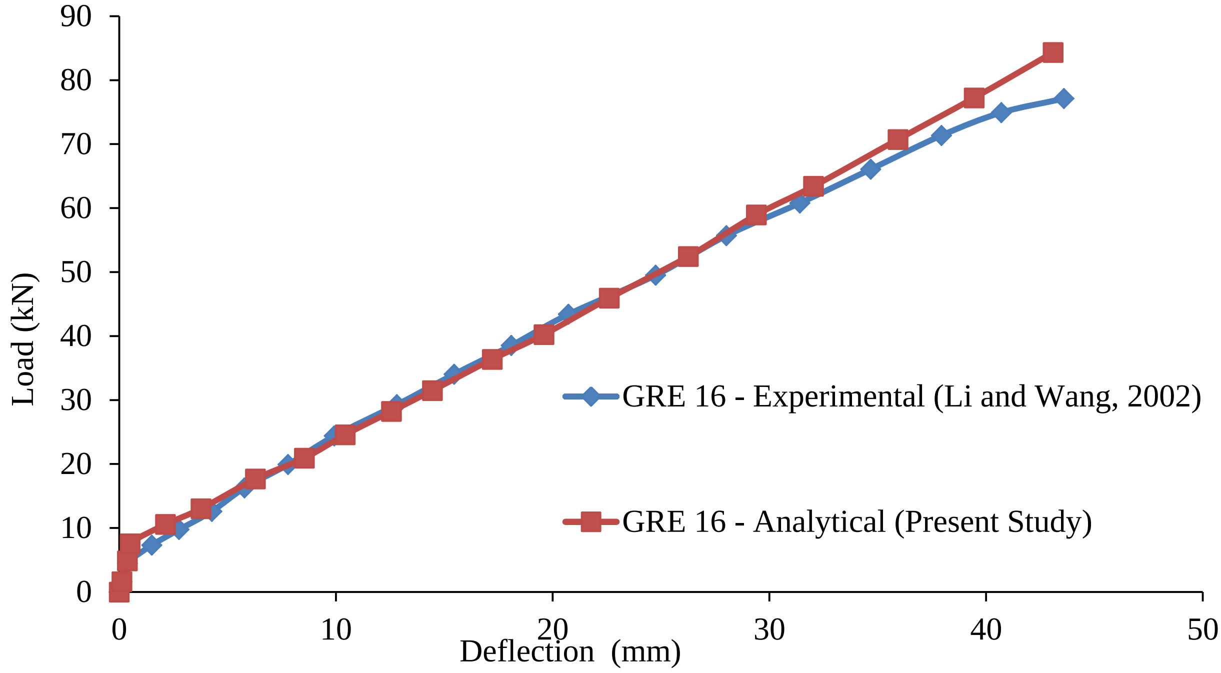

Figure 6. Comparison of Load-Deflection of beam specimen GRE 16-3R . Source: Self-elaboration.

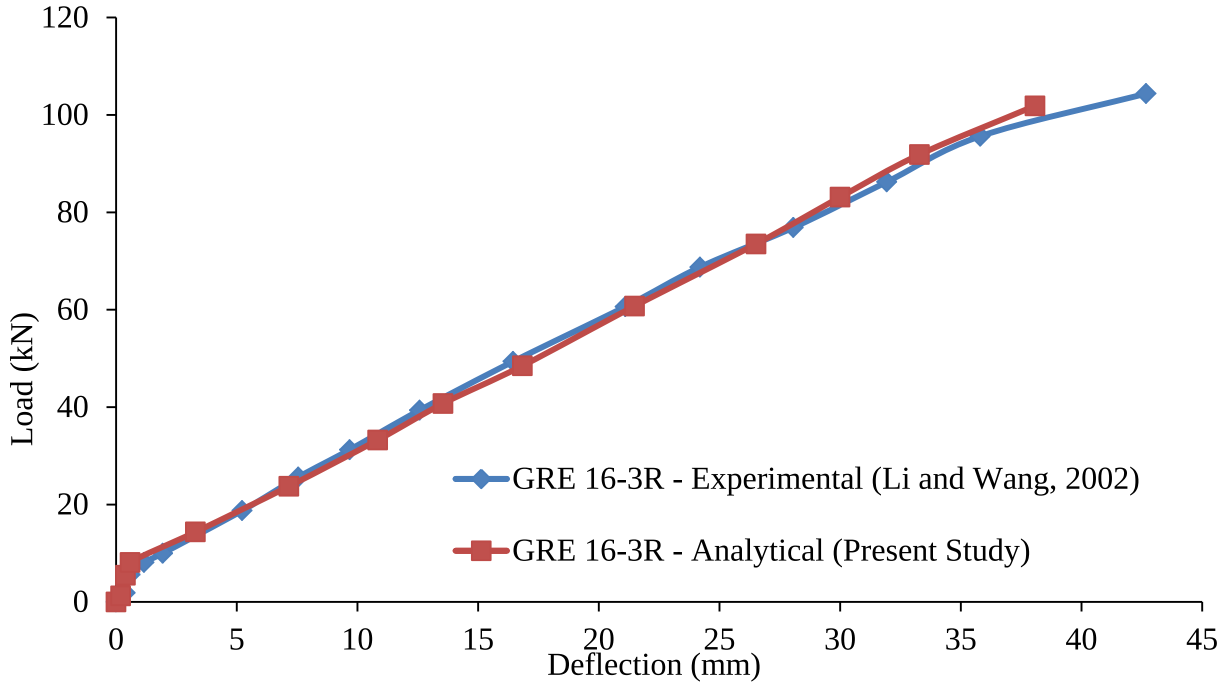

Figure 7. Comparison of Load-Deflection of beam specimen BRE 20 . Source: Self-elaboration.

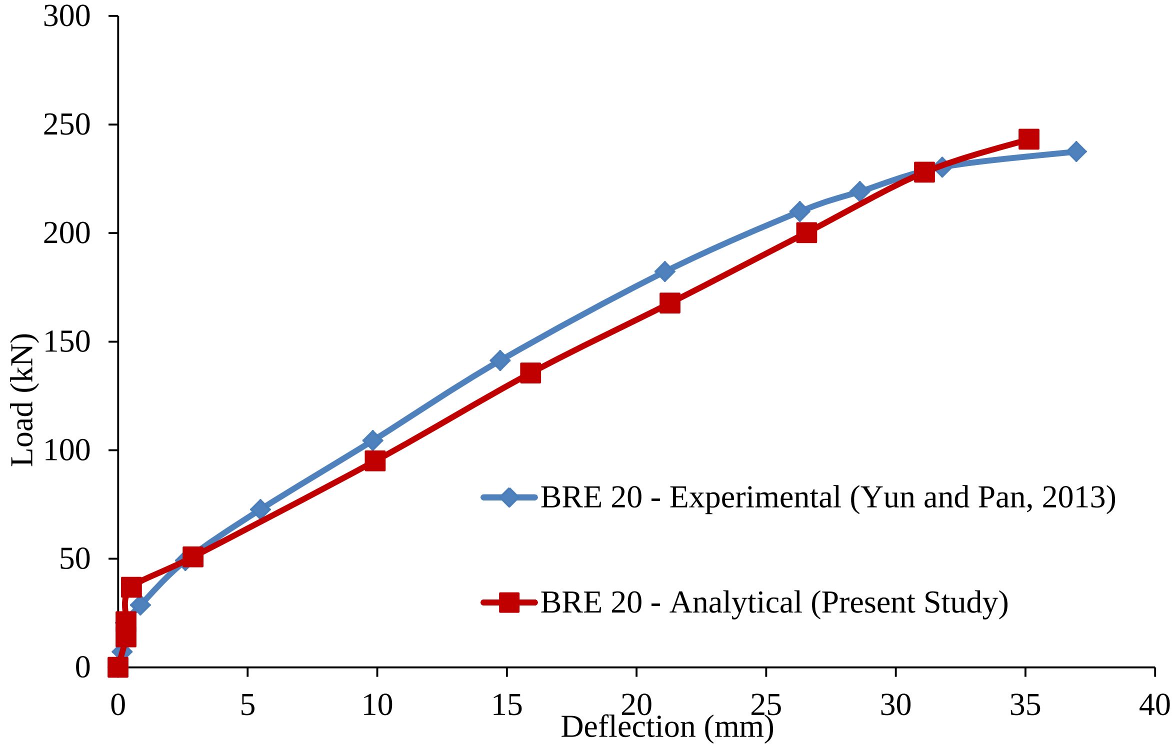

Conclusions

Based on the present investigation on FRP reinforced ECC beams, the following conclusions can be drawn:

(1) New design oriented stress-strain relationships are developed for ECC in tension and compression. The simplified stress block parameters which are derived from the developed stress-strain models are producing close agreement against experimental flexural response.

(2) Close agreement between analytical and experimental result for three different beam specimens shows the robustness of the developed stress-strain models.

(3) Hence, it is inferred that the developed stress-train models can be used for various analysis and design of ECC structural elements.

Acknowledgement

This paper is a part of the author's PhD research work which was supported by a sponsored research project (No. SR/S3/MERC/25/2007) from the Department of Science and Technology (DST), Govt. of India sanctioned to the second author.

Han, T.-S., Feenstra, P. H., & Billington, S. L. (2003). Simulation of Highly Ductile Fiber-Reinforced Cement-Based Composite Components Under Cyclic Loading. *American Concrete Institute*, *100*(6), 749–757.

Kanda, T., & Li, V. C. (1999). New Micromechanics Design Theory for Pseudostrain Hardening Cementitious Composite. *Journal of Engineering Mechanics*, 125(4), 373–381.

Li, V. C., & Lepech, M. (2006). General Design Assumptions for Engineered Cementitious Composites (ECC). In *International RILEM Workshop on High Performance Fiber Reinforced Cementitious Composites in Structural Applications* (pp. 269–277). Honolulu.

Li, V. C., & Wang, S. (2002). Flexural behaviors of glass fiber-reinforced polymer (GFRP) reinforced engineered cementitious composite beams. *ACI Materials Journal*, *99*(1), 11–21.

Maalej, M., & Li, V. C. (1995). introduction of strain-hardening engineered cementitious composites in design of reinforced concrete flexural member. *ACI Materials Journal*, *92*(2), 167–176.

Pan, J. L., & Yuan, F. (2013). Experimental study on flexural behaviors of engineered cementitious composite beams reinforced with FRP bars. In *VIII International Conference on Fracture Mechanics of Concrete and Concrete Structures FraMCoS-8* (pp. 1–11). Toledo.

Rokugo, K., Kunieda, M., Kamada, T., Fujimoto, Y., & Furukawa, K. (2002). Structural applications of strain hardening type DFRCC as tension carrying material. In *Proceedings of the JCI International Workshop on Ductile Fiber Reinforced Cementitious Composites (DFRCC)* (pp. 249–258). Tokyo.

Singh, S. B. (2015). *Analysis and Design of FRP Reinforced Concrete Structures* (First). New York: McGraw-Hill Education.